

Evolution of the ionic polarization in multiple sequential ionization: general equations and an illustrative example

Elena V. Gryzlova and Alexei N. Grum-Grzhimailo

Skobeltsyn Institute of Nuclear Physics, Lomonosov Moscow State University, 119991 Moscow, Russia *

Maksim D. Kiselev

Skobeltsyn Institute of Nuclear Physics, Lomonosov Moscow State University, 119991 Moscow, Russia *

Faculty of Physics, Lomonosov Moscow State University, Moscow 119991, Russia and

Laboratory for Modeling of Quantum Processes, Pacific National University, 680035 Khabarovsk, Russia

Maria M. Popova

Skobeltsyn Institute of Nuclear Physics, Lomonosov Moscow State University, 119991 Moscow, Russia * and

Faculty of Physics, Lomonosov Moscow State University, Moscow 119991, Russia

(Dated: July 26, 2022)

The modern Free-Electron-Lasers generate a highly intense polarized radiation which initiate a sequence of ionization and decay events. Their probability depends on the polarization of each state as function of time. Its complete accounting is limited by the fact that a state can be formed in various ways. Here we present the equivalent of rate equations for population that completely accounts polarization of radiation and formulated in terms of the statistical tensors. To illustrate our approach we theoretically consider sequential photoionization of krypton by an intense extreme ultraviolet femtosecond pulse for the photon energies below the $3d$ -shell excitation threshold. The calculations of the ion yields, photoelectron spectra and ionic polarization for various photon fluence are presented and role of polarization is discussed.

I. INTRODUCTION

When an atom is irradiated by intense electromagnetic field generated by free-electron laser (FEL) operating in the extreme ultraviolet (XUV), the first photoionization act initiates the variety of competitive processes, such as sequential ionization, Auger decay, radiation decay and others. The sample evolution depends on the radiation parameters: intensity, pulse duration and polarization. The last is often left behind the scenes, in particular, because accounting for the polarization increases number of degrees of freedom enormously. The knowledge about charge and state evolution of an irradiated sample is crucially important for a number of applications such as modeling the radioactive damage of biological samples for coherent diffraction imaging and as a fundamental test of the photoionization description basis [1, 2].

Multiple ionization of atoms by FELs has been subject of numerous and extensive investigations since the first observation at the Free-electron LASer in Hamburg (FLASH) [3]. Roughly multiple ionization may proceed in the two regimes: (a) strong field regime involving multiphoton direct single or multiple ionization [4–7]; and (b) multiphoton sequential regime proceeding with creation and subsequent ionization of different intermediate ion(s) with their possible excitation to discrete or autoionizing states [8–18]. Current research belongs to the second group. In general, both regimes may co-exist and question to attribute a process to the first regime or to the

second depends on a region of a considered photoelectron spectrum rather than on the pulse parameters.

One of the advantage of FELs is that generated radiation is highly polarized either linearly or circularly. There are a variety of researches devoted to an appearance of the polarization effects in the differential observable characteristics of sequential ionization: from photo-electron angular distribution [16, 19–22] and angular correlation [15, 23] up to recent realization of *complete/perfect* experiment [17] or ion-ion correlation [7]. We are not aware about angle-resolved experiments proceeding with forming more than triple-charged ions [20, 24].

On the other side, there are many researches of polarization effects in integral cross-section mainly in a integral linear or circular dichroism within pump-probe scheme [25–30]. Polarization of an ionized state may appear as variation of ionization probability up to complete suppression. The dynamically quasiforbidden transitions in photoionization of pumped open-shell atoms were found and interpreted [31].

In spite of numerous investigations of dichroism have shown that polarization may affect integral characteristics such as ionic yield and photoelectron spectrum, to the best of our knowledge there are no studies investigating multiple ionization with complete accounting of intermediate states polarization. These type of researches is quite resource-consuming because they suppose to solve a system of the rate equations for all affected magnetic sublevels instead of having one equation for one state that increase number of equations significantly [32]. Therefore, most of researches use relevant ionization/excitation cross sections by polarized radiation neglecting influence of sub-sequined steps to former one which may cause de-

* gryzlova@gmail.com

pletion of target magnetic sub-levels.

In the manuscript we developed method suitable for an atom (ion) in linearly or circularly polarized radiation under assumption that the levels are separated and populated incoherently. The method is based on solution the system of equations for statistical tensors similar to the system of rate equations for populations which is widely used in the description atom-field interactions [33–41] but presented in terms of statistical tensors.

As an illustrative example we consider sequential ionization of krypton by electromagnetic pulse with photon energy 60–80 eV that is below the lowest excitation energy of $3d$ shell ($3d^{-1}5p[5/2]_1$ 91.2 eV [42]). For both single or double $4s$ -vacancy states the Auger decay is energetically forbidden, therefore the dominant processes govern over temporal dynamics are subsequent photoionization from the $4s$ and the $4p$ orbitals with emission of a photoelectron e_{ph} :

$$\gamma + \text{Kr}^{n+} 4s^k 4p^m \longrightarrow \begin{cases} \text{Kr}^{(n+1)+} 4s^{k-1} 4p^m + e_{ph} \\ \text{Kr}^{(n+1)+} 4s^k 4p^{m-1} + e_{ph} \end{cases} \quad (1)$$

Relaxation of $4s$ -vacancies proceeds via radiative transition from the $4p$ to the $4s$ level with fluorescence of a photon γ_{fl}

$$\text{Kr}^{n+} 4s^k 4p^m \longrightarrow \text{Kr}^{n+} 4s^{k+1} 4p^{m-1} + \gamma_{fl} \quad (2)$$

We consider relatively short femtosecond pulses and the relaxation transitions can be neglected.

Sequential ionization from neutral Kr to the triply charged ion Kr^{3+} involving $4s$ and $4p$ shells of Kr and its ions is shown in Figure 1, where the configurations, terms and relative energies are indicated. The additional details needed for interpretation of the photo-electron spectrum are presented in Table I. We neglect fine-structure splitting, do not include shake-up, direct two-photon and one-photon double ionization channels [43] and consider the sequential ionization up to triple three-photon ionization exactly in the same setup as we did in [44] for *unpolarized* radiation.

In the next section we outline a theoretical approach for modeling the atom-field interaction based on the solution of a system of the rate equations for statistical tensors. In Section III, we present throughout analysis of the ionic polarization. In Section IV, the results on the time evolution of the Kr target under the FEL pulse (ionic yields) and the resulting photoelectron spectra are presented and discussed. We use atomic units until otherwise indicated.

II. SYSTEM OF EQUATIONS FOR EVOLUTION OF THE STATISTICAL TENSORS

The goal of this section is to formulate equivalent of rate equations accounting polarization of the states in terms of the statistical tensors for linearly and circularly

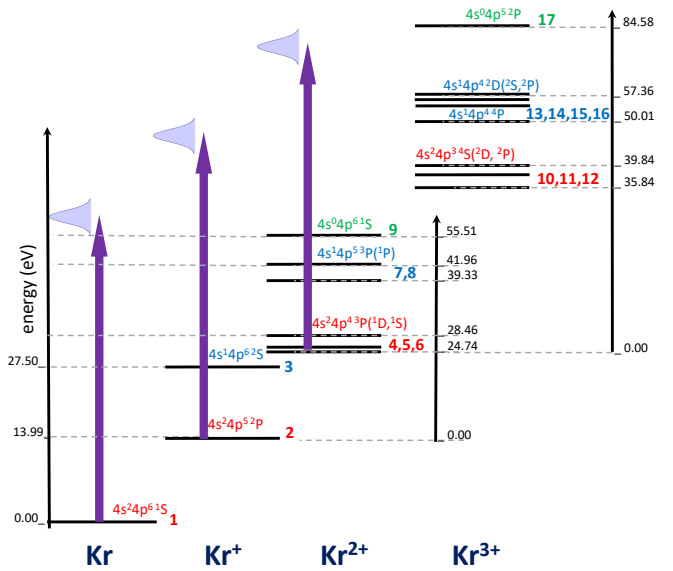


FIG. 1. The scheme of transitions in sequential multiphoton ionization of Kr. The experimental ionization thresholds were taken from [45] and averaged over a multiplet.

polarized radiation in dipole approximation. Under these conditions statistical tensor of photons $\rho_{k\gamma q_\gamma} \neq 0$ for $q_\gamma = 0$ and $k_\gamma \leq 2$, and leaving treating of an electron-ionic correlation out, only zero rank statistical tensors of an electron $\rho_{k_e=0, q_e=0}$ exist. Therefore all non-zero statistical tensors of ionic states have projection $q = 0$.

It is well established [46, 47] that if a state i of a n -charged ion A^{n+} with total angular momentum J_i absorbs a (dipole) photon and ionizes into a state f of $A^{(n+1)+}$ with total momentum J_f , the statistical tensors of initial $\rho_{k_i 0}(J_i)$ and final $\rho_{k_f 0}(J_f)$ states are connected by the equation:

$$\rho_{k_f 0}(J_f) = \sum_{k_\gamma} \rho_{k_i 0}(J_i) S[k_i, k_\gamma, k_f], \quad (3)$$

where transition parameter $S[k_i, k_\gamma, k_f]$ is presented in terms of reduced ionization amplitudes as

$$S[k_i, k_\gamma, k_f] = 4\pi^2 \alpha \omega \rho_{k_\gamma 0} B[k_i, k_\gamma, k_f]; \quad (4)$$

$$B[k_i, k_\gamma, k_f] = \hat{k}_i \hat{k}_\gamma (k_i 0, k_\gamma 0 | k_f 0) \frac{\hat{J}_f}{\hat{J}_i} (-1)^{J_f + k_f} \sum_{j J' J''} \hat{J} \hat{J}' (-1)^{J'+j} \left\{ \begin{array}{c} J_f & J_f & k_f \\ J & J' & j \end{array} \right\} \left\{ \begin{array}{c} J_i & 1 & J \\ J_i & 1 & J \end{array} \right\}_{k_i k_\gamma k_f} \langle (J_f j) J || \hat{D} || J_i \rangle \langle (J_f j) J' || \hat{D} || J_i \rangle^*. \quad (5)$$

Here $\hat{a} = \sqrt{2a+1}$, \hat{D} is the operator of the atomic electric dipole momentum, and usual notation for Clebsch-Gordan coefficients, 6j- and 9j-symbols are used. Throughout the manuscript we use non-conventional nor-

malization of the statistical tensors: if state J_a is completely populated, $\rho_{00}(J_a) = 1$ (instead $\rho_{00}(J_a) = 1/\hat{J}_a$) that allows to consider zero rank statistical tensors as population in percents (summed over all states population $\sum_a \rho_{00}(J_a) = 1$). Parameter $S[0, 0, 0]$ is the ionization cross-section of an unpolarized state with J_i to an ion with J_f .

The transparent way to get time-dependent form of (3) is to start with conventional rate equations for the level populations:

$$\frac{dN_{aM_a}(t)}{dt} = j(t) \sum_{\substack{b \neq a, M_b \\ b \\ k \\ k}}^L [\sigma_{bM_b \rightarrow aM_a} N_{bM_b}(t) - \sigma_{aM_a \rightarrow bM_b} N_{aM_a}(t)] , \quad (6)$$

where $N_{aM_a}(t)$ is the population of sublevel a with magnetic quantum number M_a and $j(t)$ is the time-dependent intensity of the incident radiation (envelope), L is the number of the accounted states, $\sigma_{aM_a \rightarrow bM_b}$ is the photoionization cross section from sublevel aM_a of Aⁿ⁺ to sublevel bM_b of A⁽ⁿ⁺¹⁾⁺ which is connected with transition parameter (4):

$$\sigma_{iM_i \rightarrow fM_f} = \hat{J}_i \sum_{\substack{k \\ k_i \\ k_\gamma \\ k_f}} (-1)^{J_i - M_i + J_f - M_f} (J_i M_i, J_i - M_i | k_i 0) (J_f M_f, J_f - M_f | k_f 0) S[k_i, k_\gamma, k_f] . \quad (7)$$

The total ionization cross section of an unpolarized state by unpolarized radiation is an averaged sum of cross sections from magnetic sublevels:

$$\sigma = \frac{\sum_{M_i M_f} \sigma_{iM_i \rightarrow fM_f}}{2J_i + 1} \equiv S[0, 0, 0] . \quad (8)$$

The statistical tensor corresponding to a state a is constructed from its population $N_{aM_a}(t)$ straightforward by the definition:

$$\rho_{k_a 0}(J_a) = \hat{J}_a \sum_{M_a} (-1)^{J_a - M_a} (J_a M_a, J_a - M_a | k_a 0) N_{aM_a} ; \quad (9)$$

$$N_{aM_a} = \frac{1}{\hat{J}_a} \sum_{k_a} (-1)^{J_a - M_a} (J_a M_a, J_a - M_a | k_a 0) \rho_{k_a 0}(J_a) \quad (10)$$

Collecting the all above, we are now able to write down the analogue of the rate equations (6) in terms of statistical tensor:

$$\frac{d\rho_{k_a 0}(J_a)}{dt} = \left. \frac{d\rho_{k_a 0}(J_a)}{dt} \right|_{\text{in}} - \left. \frac{d\rho_{k_a 0}(J_a)}{dt} \right|_{\text{out}} , \quad (11)$$

where the term describing pumping of population ($b = i$ is initial, $a = f$ is final) is quite simple:

$$\begin{aligned} \left. \frac{d\rho_{k_a 0}(J_a)}{dt} \right|_{\text{in}} &= j(t) \hat{J}_a \sum_{M_a b M_b} (-1)^{J_a - M_a} (J_a M_a, J_a - M_a | k_a 0) \sigma_{bM_b \rightarrow aM_a} N_{bM_b} \\ &= j(t) \sum_{\substack{M_a b M_b \\ k'_a k'_\gamma k'_b k'_f}} (J_a M_a, J_a - M_a | k_a 0) (J_a M_a, J_a - M_a | k'_a 0) (J_b M_b, J_b - M_b | k_b 0) (J_b M_b, J_b - M_b | k'_b 0) S[k_b, k'_\gamma, k'_b] \rho_{k'_b 0}(J_b) \\ &= j(t) \sum_{k'_\gamma b k_b} S[k_b, k'_\gamma, k_a] \rho_{k_b 0}(J_b) . \end{aligned} \quad (12)$$

The term describing the leaking of population ($a = i$

is initial, $b = f$ is final) is much more trickier:

$$\begin{aligned} \left. \frac{d\rho_{k_a 0}(J_a)}{dt} \right|_{\text{out}} &= j(t) \hat{J}_a \sum_{M_a b M_b} (-1)^{J_a - M_a} (J_a M_a, J_a - M_a | k_a 0) \sigma_{aM_a \rightarrow bM_b} N_{aM_a} \\ &= j(t) \frac{\hat{J}_a}{\hat{J}_b} \sum_{\substack{M_a b M_b \\ k'_a k''_a k'_\gamma k'_b}} (-1)^{J_a - M_a} (J_a M_a, J_a - M_a | k_a 0) (J_a M_a, J_a - M_a | k'_a 0) (J_a M_a, J_a - M_a | k''_a 0) \\ &\quad (-1)^{J_b - M_b} (J_b M_b, J_b - M_b | k_b 0) S[k'_a, k'_\gamma, k_b] \rho_{k''_a 0}(J_a) \\ &= j(t) \hat{J}_a \sum_{k'_a k''_a k'_\gamma} (-1)^{k''_a} \hat{k}'_a (k_a 0, k'_a 0 | k''_a 0) \left\{ \begin{array}{c} k_a \\ J_a \\ k'_a \\ J_a \\ k''_a \\ J_a \end{array} \right\} S[k'_a, k'_\gamma, 0] \rho_{k''_a 0}(J_a) . \end{aligned} \quad (13)$$

The feature of this equation is that, while in the rate

equations for population decreasing of a population is

always proportional to it, in the rate equations for statistical tensors decreasing of a tensor depends on other tensors of the state.

Having the equations (11)–(13), one can solve the system for statistical tensors which is completely similar to the conventional rate equations apart from the specific form of the coefficients. The advantage of this approach is that with more states are involved, the size of system (11) increases slower than the size of system (6) where magnetic quantum numbers are directly accounted. In our case (see Table I) $L = 17$, the number of magnetic sublevels is $\sum_a (2J_a + 1) = 45$, the number of statistical tensors is 31.

Time-dependent alignment and orientation of an ion are the ratio of the corresponding statistical tensors:

$$A_2(J_f) = \frac{\rho_{20}(J_f)}{\rho_{00}(J_f)}, \quad A_1(J_f) = \frac{\rho_{10}(J_f)}{\rho_{00}(J_f)}. \quad (14)$$

For forthcoming discussion let's introduce conventional *stationary* alignment of a state f :

$$\mathcal{A}_f = \frac{-\sqrt{2}B[0, 2, 2] + \mathcal{A}_i(B[2, 0, 2] - \sqrt{2}B[2, 2, 2])}{B[0, 0, 0] - \sqrt{2}B[2, 2, 0]} \quad (15)$$

By *stationary* alignment we named the alignment obtained in some branch $i \rightarrow f$ neglecting all other pathways as well as depletion/saturation of the considered state.

There are maximal and minimal values of an alignment directly following from the statistical tensor definition:

$$A_2(J) = \frac{\sum_M (-1)^{J_M} (JM, J-M | 20) N_{JM}}{\sum_M (-1)^{J_M} (JM, J-M | 00) N_{JM}}, \quad (16)$$

that gives:

$$A_2(P) = \frac{1}{\sqrt{2}} \frac{N_{11} + N_{1-1} - 2N_{10}}{N_{11} + N_{1-1} + N_{10}}, \quad (17)$$

$$A_2(D) = \sqrt{\frac{10}{7}} \frac{N_{22} + N_{2-2} - (N_{21} + N_{2-1})/2 - N_{20}}{N_{22} + N_{2-2} + N_{21} + N_{2-1} + N_{10}} \quad (18)$$

It is obvious that for P -term states maximal and minimal alignment is $1/\sqrt{2}$ and $-\sqrt{2}$, correspondingly (17); for D -term they are $\sqrt{10/7}$ and $-\sqrt{10/7}$ (18).

The Gaussian distribution of the incident *photon flux density* is assumed:

$$j(t) = j_0 \exp(-t^2/t_p^2), \quad (19)$$

thus the pulse full width at half maximum $\text{FWHM} = 2\sqrt{\ln 2} t_p$. The integral number of photons per 1 \AA^2 in the entire pulse i.e. *fluence* F is related to the intensity as

$$j_0 = \frac{2\sqrt{\ln 2} F}{\sqrt{\pi} \text{ FWHM}} = 0.0063634 \frac{F [\text{ph}/\text{\AA}^2]}{\text{FWHM [fs]}}. \quad (20)$$

The typical pulse duration obtained at the seeded FEL FERMI [48, 49] is around 50–100 fs; we set the pulse duration to $t_p = 60$ fs ($\text{FWHM} = 100$ fs).

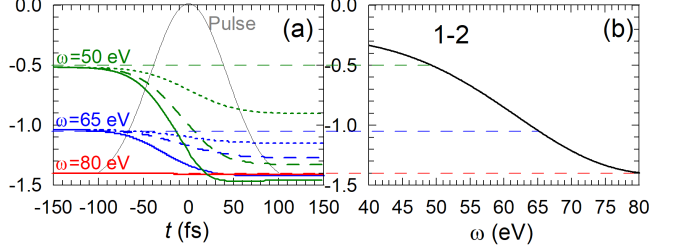


FIG. 2. (a) The alignment of $\text{Kr}^+ 4s^2 4p^5 2P$ ion calculated as function of time at $\omega = 50, 65$ and 80 eV. The solid, dashed and dotted lines correspond to fluence $F = 3000, 1000$ and 400 ph/ \AA^2 . (b) Conventional alignment of the same ion as function of energy (accounting difference in definitions this data are in accordance with [51]). Here '1-2' and after 'a-b' indicates the transition between the states labeled according to Table I.

III. ANALYSIS OF THE IONS ALIGNMENT

Photoionization cross sections of $4s^k 4p^m 2S+1L$ multiplets for Kr ions in different charge states were calculated by means of the B-spline R-matrix code [50]. For each of the ionization steps the basis wave functions of the initial nine and the final seventeen states listed in Table I were obtained in the way described in [44], where one can also find the photoionization cross sections curves for each step and comparison with another theories and experiments for neutral krypton ionization.

Figure 2 illustrates the main idea of the investigation: to account dynamical change of polarization and its impact to the observable values. It shows alignment of the 'first' ion $\text{Kr}^+ 4s^2 4p^5 2P$ as function of time (eqn. 14) and its stationary alignment (eqn. 15). The conventional alignment (figure 2(b)) as function of energy has a broad maximum of absolute value caused by Cooper minimum of $4p \rightarrow \varepsilon d$ ionization amplitude. At the Cooper minimum alignment approaches to $-\sqrt{2}$ that is minimal possible value allowed by eqn. (17). One can see (figure 2(a)) that at the pulse beginning the alignment is equal to the conventional value at corresponding photon energy: -0.5 ($\omega = 50$ eV), -1 ($\omega = 65$ eV) and -1.41 ($\omega = 80$ eV). Then as linearly polarized pulse ionizes the ion preferably from $|m| = 1$, the alignment tends to get stronger, and it is clearly seen for $\omega = 50$ and $\omega = 65$ eV. Moreover, originally smaller alignment at $\omega = 50$ eV may became stronger than at $\omega = 65$ eV due to dynamical effects. At $\omega = 80$ eV the tendency is suppressed by the complete depletion of $|m| = 1$ sublevels.

Figure 3 shows stationary alignment (eqn. 15) of the other ions assuming that they are created from an *unpolarized* state $\mathcal{A}_i = 0$. There are three types of features one can see: (a) the series of sharp structures at the lower-energy edge; (b) deep minima or high maxima placed around $\omega = 80$ eV; (c) no energy dependency for some ionization pathways.

(a) The sharp structures emerge due to Rydberg auto-

TABLE I. List of the pathways in sequential three-photon ionization of Kr within the LS-coupling scheme. The columns and lines correspond to the initial and final states of the pathway, respectively. We denote different transitions contributed to a one photoelectron line by a capital letter. Numbers are experimental ionization thresholds [45] for the corresponding transitions in eV, averaged over a multiplet. Unmarked transitions are weak and their contribution to the photoelectron spectra is negligible.

N	Initial State	$4s^2 4p^6 1S$	$4s^2 4p^5 2P^o$	$4s^1 4p^6 2S$	$4s^2 4p^4 3P$	$4s^2 4p^4 1D$	$4s^2 4p^4 1S$	$4s^1 4p^5 3P^o$	$4s^1 4p^5 1P^o$	$4s^0 4p^6 1S$
	Final State									
1	$4s^2 4p^6 1S$	-	-	-	-	-	-	-	-	-
2	$4s^2 4p^5 2P^o$	A, 14.0	-	-	-	-	-	-	-	-
3	$4s^1 4p^6 2S$	E, 27.5	-	-	-	-	-	-	-	-
4	$4s^2 4p^4 3P$	-	B, 24.4	-	-	-	-	-	-	-
5	$4s^2 4p^4 1D$	-	D, 26.2	-	-	-	-	-	-	-
6	$4s^2 4p^4 1S$	-	F, 28.5	-	-	-	-	-	-	-
7	$4s^1 4p^5 3P^o$	-	I, 38.7	C, 25.2	-	-	-	-	-	-
8	$4s^1 4p^5 1P^o$	-	K, 42.0	F, 28.4	-	-	-	-	-	-
9	$4s^0 4p^6 1S$	-	-	K, 42.1	-	-	-	-	-	-
10	$4s^2 4p^3 4S^o$	-	-	-	G, 35.8	-	-	-	-	-
11	$4s^2 4p^3 2D^o$	-	-	-	J, 38.0	H, 36.1	33.8	-	-	-
12	$4s^2 4p^3 2P^o$	-	-	-	K, 39.7	I, 37.9	G, 35.6	-	-	-
13	$4s^1 4p^4 4P$	-	-	-	M, 50.6	-	-	G, 35.5	-	-
14	$4s^1 4p^4 2D$	-	-	-	O, 53.9	N, 52.1	49.8	J, 38.8	H, 36.3	-
15	$4s^1 4p^4 2S$	-	-	-	S, 57.4	Q, 55.6	53.3	L, 42.3	K, 39.8	-
16	$4s^1 4p^4 2P$	-	-	-	R, 56.4	P, 54.6	N, 52.3	L, 41.4	J, 38.8	-
17	$4s^0 4p^5 2P^o$	-	-	-	-	-	P, 54.9	N, 52.3	J, 38.7	-

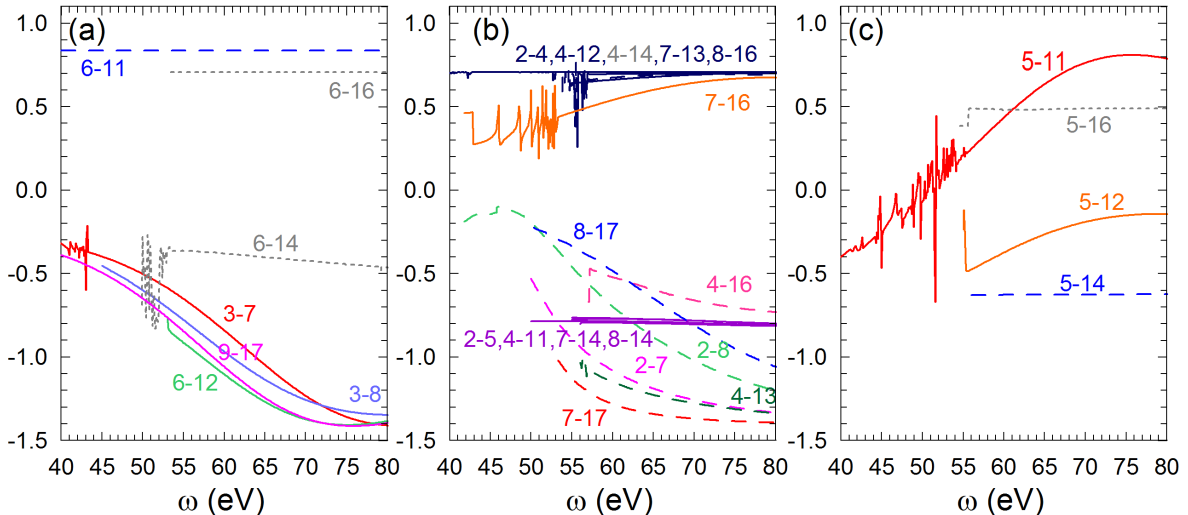


FIG. 3. Stationary alignment as function of energy for different ionization pathways: (a) from ions with $4s^n 4p^m 2S_i+1 S$ term, (b) from $4s^n 4p^m 2S_i+1 P$ term, (c) from $4s^n 4p^m 2S_i+1 D$ term.

ionization series and observed in all spectra except ones corresponding to highest allowed threshold, e.g. 1 – 3, 2 – 8, 3 – 9, {4, 5, 6} – 16, {7, 8, 9} – 17. The resonance structure is hardly resolved in the modern experiments and therefore it is not a subject of current investigation. Here we cut off most of the resonances leaving a few just for illustration.

(b) The minima and maxima are connected with the Cooper minimum in $4p \rightarrow \varepsilon d$ ionization amplitudes. Note that most of them are quite close to the allowed limits: $-\sqrt{2}$ and $1/\sqrt{2}$ for P -terms (eqn. 17) and $\pm\sqrt{7}/10$

for D -terms (eqn. 18).

(c) Weak dependency on energy is explained by domination of a particular channel. In order to explore the issue further it is constructive to present eqn. (5) in simpler form via single-electron transition amplitude $d_{l_i l}$ from l_i -shell to εl -continuum i.e. neglecting term dependency of

the amplitudes:

$$\bar{B}[k_i, k_\gamma, k_f] = \hat{k}_i \hat{k}_\gamma (k_i 0, k_\gamma 0 | k_f 0) \hat{L}_i \hat{L}_f (-1)^{k_\gamma} \sum_l \left\{ \begin{array}{c} 1 \ 1 \ k_\gamma \\ l_i \ l_i \ l \end{array} \right\} \left\{ \begin{array}{c} l_i \ L_i \ L_f \\ l_i \ L_i \ L_f \\ k_\gamma \ k_i \ k_f \end{array} \right\} |d_{l_i l}|^2. \quad (21)$$

We will address to this simplification as *no correlation* NC-model.

Ionized shell is $l_i = 4s$. Within NC-model $L_i = L_f$ and polarization of an initial state simply transfers to a final ion: $\mathcal{A}_f = \mathcal{A}_i$. That means that non-zero alignment of these branches (marked by dashed lines in figure 3) is result of the correlation effects originating from strong term mixing. Moreover, branches 4 – 14, 4 – 15, 5 – 15, 5 – 16, 6 – 14, 6 – 16 are not allowed in the simple NC-model at all, because without correlation ionization of s-shell cannot change term of an ion. Their cross-sections are much lower than others [44]. Branch 6 – 16 is governed by eqn. (15) and (5) and only allowed due to the correlations channel $\langle ^2P \varepsilon p^1P || \hat{D} || ^1S \rangle$ leads to $\mathcal{A}_f = 1/\sqrt{2}$.

Ionized shell is $l_i = 4p$. Lets introduce $\kappa = |d_{pd}|^2/|d_{ps}|^2$ and re-arrange eqn. (15) using (21) as:

$$\mathcal{A}_f = -\sqrt{2} \frac{1 + \frac{\kappa}{10}}{1 + \kappa}, \quad \begin{array}{c} L_i=S \\ L_f=P \end{array}, \quad (22)$$

$$\mathcal{A}_f = \frac{\frac{1}{\sqrt{2}}(1 + \frac{\kappa}{10}) + \mathcal{A}_i(\frac{1}{2} - \frac{2}{5}\kappa)}{1 + \kappa + \mathcal{A}_i/\sqrt{2}(1 + \frac{\kappa}{10})}, \quad \begin{array}{c} L_i=P \\ L_f=P \end{array}, \quad (23)$$

$$\mathcal{A}_f = -\sqrt{\frac{7}{10}} \frac{1 + \frac{\kappa}{10} - \mathcal{A}_i \sqrt{2}(\frac{5}{14} + \frac{17}{35}\kappa)}{1 + \kappa - \mathcal{A}_i \frac{\sqrt{2}}{10}(1 + \frac{\kappa}{10})}, \quad \begin{array}{c} L_i=P \\ L_f=D \end{array}. \quad (24)$$

Equation (22) governs 1 – 2, 3 – 7, 3 – 8, 6 – 12, 9 – 17 branches. They generally demonstrate essential energy-dependence because of interplay between d_s and d_d amplitudes (see figure 3(a)). Branch 6 – 11 is not allowed in NC-model, governed by eqn. (15) and (5), hence the alignment determined by the only allowed channel $\langle ^2D \varepsilon d^1P || \hat{D} || ^1S \rangle$ is $\mathcal{A}_f = \sqrt{7/10}$.

Equation (23) governs 2 – 4, 4 – 12, 7 – 13, 7 – 16, 8 – 16 branches. All of them practically independent on energy and very close to $\mathcal{A}_f = 1/\sqrt{2}$ indicating domination of s-wave ($\kappa \approx 0$). The same is correct for 2 – 5 and 4 – 11 governed by eqn. (24): for them alignment values are close to $\mathcal{A}_f = -\sqrt{7/10}$.

In figure 3 all of initial states are supposed to be unpolarized. *Ab initio* it is correct only for S-terms (panel a). Below we discuss how panels b and c affected by polarization.

Equation (23) shows that while κ is small $P – P$ ionization causes the maximal possible positive alignment $\mathcal{A}_f = 1/\sqrt{2}$ independently on alignment of initial state. But the closer polarization of initial state \mathcal{A}_i to $-\sqrt{2}$ the lower s-wave contribution, finally at $\mathcal{A}_i = -\sqrt{2}$ s-wave contributions are completely compensated both in numerator and denominator and the channel is closed. At

this situation (as well as if d -wave dominates) alignment of final state tends to edge negative value $\mathcal{A}_f = -\sqrt{2}$.

Equation (24) shows that where s-wave dominates the alignment of final state varies from $\mathcal{A}_f = -\sqrt{10/7}$ (minimal possible) at initial state $\mathcal{A}_i = -\sqrt{2}$ to twice smaller $\mathcal{A}_f = -\sqrt{5/14}$ at $\mathcal{A}_i = 1/\sqrt{2}$. At negative \mathcal{A}_i d -wave weakly modifies the alignment because works "to the same side" (sign before κ is always positive). For example at $\mathcal{A}_i = -\sqrt{2}$ ratio \mathcal{A}_f at $\kappa = 0$ (s-wave dominates) and \mathcal{A}_f at $\kappa \rightarrow \infty$ (d -wave dominates) is $25/22 \approx 1.14$.

From the above one can see that while the NC-model describes ionization from valence 4p-shell pretty well, it completely fails for 4s-shell indicating much stronger correlations in ionization of the sub-valence shell.

IV. RESULTS AND DISCUSSION

In this section we present and discuss results for observable values: population of different ionic species (fig. 4), ionic yields (fig. 5) and photoelectron spectra (fig. 6). As was discussed in [44], the curves in figures 4–6 remain the same for fixed values of fluence F if we change pulse duration and do appropriate scaling of the timescale. The reason of the scaling is absence of any natural timetick (like the Auger decay) in the system under consideration.

A. The ionic yields

In figure 4 we present results for linearly polarized and unpolarized radiation at two photon energies (65 eV and 80 eV) and fluence $F = 1000 \text{ ph}/\text{\AA}^2$ corresponding to intensity $2.2 \cdot 10^{15} \text{ W/cm}^2$ (at $t_p = 60 \text{ fs}$). We present population as a function of time summed up within one configuration over possible terms.

The concentration of neutral atoms monotonically decreases with time (figure 3(a,b)). The number of singly and doubly charged ions first increases with time, but then it may drop down (figures 3(c,d)), because of their further ionization to Kr^{3+} . The last monotonically increases with time (figure 3(e,f)). At any time the sum of all populations presented in figure 4 corresponding to the same fluence, photon energy and polarization equals unity.

At first step (figure 4(a,b)) the alignment of $\text{Kr}^+ 4s^2 4p^5 2P$ ion (red curves) prevents its further ionization triply increasing its final population. In low intensity regime this tendency would keep: polarization of an ion should simply suppress some of ionization channels, leaving the other channels unaffected. If intensity is high enough to involve the saturation and depletion effects the tendency violates. For example, alignment increases number of double 4s-hole $\text{Kr}^{2+} 4s^0 4p^6 1S$ ions (green lines in figure 4(c)) in spite of the ions are created in the pathway affecting only S-terms. The tendency is also relevant

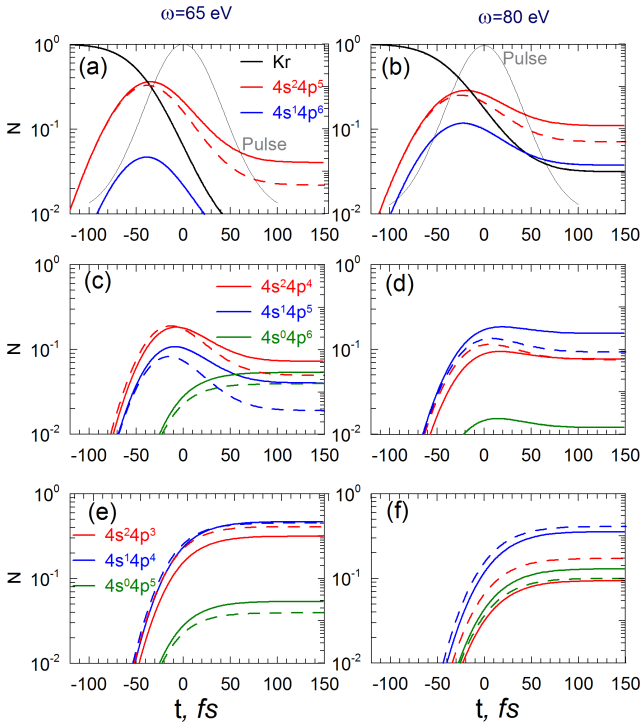


FIG. 4. Population of the different ion charge states and configurations for fluences $F = 1000 \text{ ph}/\text{\AA}^2$ at the photon energies 65 eV (a,c,e) and 80 eV (b,d,f) calculated with (solid lines) and without (dashed lines) accounting polarization of the ionic states. The population of the neutral Kr and Kr^+ , Kr^{2+} and Kr^{3+} are in the first, second and third rows. Black lines — yield of neutral Kr; red lines — yield of ions with $4s^24p^{6-n}$ configuration, where n is the ion charge; blue lines — ions with $4s^14p^{6-n+1}$ configuration, green lines — ions with $4s^04p^{6-n+2}$ configuration. The pulse envelope (grey line) is indicated in the upper panels.

for the next step (figure 4(e)) and at $\omega = 80 \text{ eV}$ corresponding higher polarization may rearrange ionic yields: for unpolarized radiation output of $4s^24p^3$ is higher than $4s^04p^5$, while for polarized radiation output of $4s^04p^5$ is higher (red and green lines in figure 4(f)).

Such a high yields of $4s$ single- and double-hole ions at $\omega = 65 \text{ eV}$ are really surprising accounting that there are the Cooper minima in $4s$ -shell ionization of both Kr and Kr^+ [44] situated in the region of 45-50 eV and, moreover, including the fact that $4s$ -ionization cross section at $\omega = 65 \text{ eV}$ is still one order of magnitude lower than $4p$ -ionization cross section.

There is the Cooper minimum in the $4p$ -shell ionization amplitude of neutral Kr near 80 eV, aside cross sections from $4p$ -ionization of other ions at $\omega = 80 \text{ eV}$ are smaller than at $\omega = 65 \text{ eV}$. As result, yield of single and double $4s$ -hole states are higher than for 65 eV (compare blue lines in figure 4(c) and 4(d), green lines in 4(e) and 4(f)). Results for the first $\text{Kr}^+4s^24p^5$ ion may look contradicted: in spite of cross section drops down by 3 times,

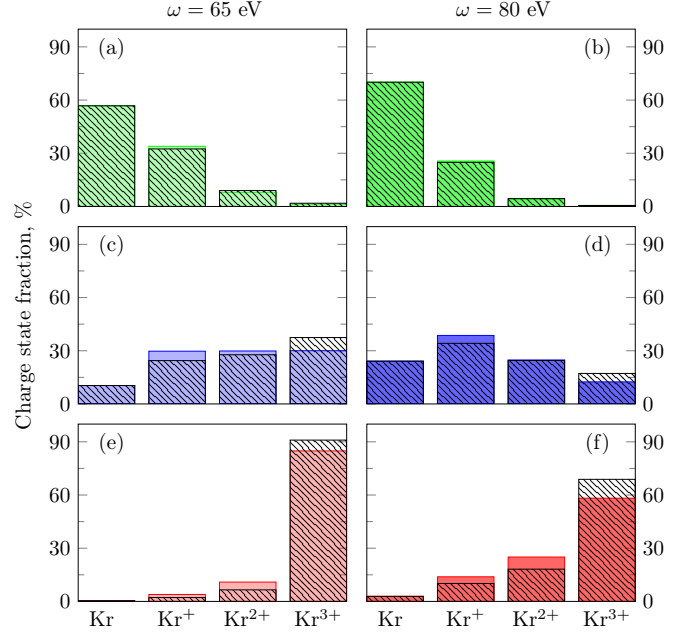


FIG. 5. The charge-state yields for three fluences: $F = 100 \text{ ph}/\text{\AA}^2$ (a,b), $F = 400 \text{ ph}/\text{\AA}^2$ (c,d), and $F = 1000 \text{ ph}/\text{\AA}^2$ (e,f) for the photon energies 65 eV (a,c,e) and 80 eV (b,d,f). The shaded areas show the results for unpolarized radiation.

the yield increases by 5 times between 65 and 80 eV (red lines in fig. 4ab). That is because very high (minimal) alignment prohibited the next ionization step, and the ions accumulated in this state.

In practice the different ionic configurations are not distinguished. In figure 5 the overall ionic yields at the fluences $F = 100 \text{ ph}/\text{\AA}^2$, $F = 400 \text{ ph}/\text{\AA}^2$ and $F = 1000 \text{ ph}/\text{\AA}^2$ and the photon energies $\omega = 65 \text{ eV}$ and $\omega = 80 \text{ eV}$ are presented. The relative populations of the different ionic states change with intensity, switching from perturbative (panels a,b) to saturation (e,f) patterns. As expected, summing over the configurations decreases difference between polarized and unpolarized cases. At lower intensity (figure 5(a,b)) there are no polarization effects, but at higher they become more essential for final Kr^{3+} ions and may decrease the ionic yield up to 10% of total ionic number (figure 5(c,e,f)).

The next step, i.e. ionization of Kr^{3+} for 80 eV photons is energetically possible and the last column in figure 5(b,d,f) actually presents the sum yield of ions with charges three and higher. Nevertheless that cannot affect presented below photoelectron spectra.

B. Photoelectron Spectra

Photoelectron spectrum can be cast as function of the probability $P_{ab}(F)$ of an ion (atom) in a state a is ionized into the ion in a state b over the entire pulse and energy

of this transition:

$$f_F(\varepsilon) = \sum_{ab} P_{ab}(F) \exp[-(\varepsilon + I_{ab} - \omega)^2/\Gamma^2], \quad (25)$$

where ε is the photoelectron kinetic energy, I_{ab} is the binding energy of ionization of the state a to the state b and Γ is the resolution of the electron detector. As in [44], we set value $\Gamma = 0.42$ eV to leave the fine structure of levels unresolved.

The photoelectron spectrum provides more detailed information on the pathways of the sequential ionization than the ion yield because it keeps memory on the relative population of the intermediate states of the process (see figure 1 and Table I).

The generated photoelectron spectra for two photon energies, 65 eV and 80 eV, are displayed in figures 6(a,c) and 6(b,d), correspondingly. We consider two values of fluence: low $F = 100 \text{ ph}/\text{\AA}^2$ (figure 6(a,b)) and high $F = 1000 \text{ ph}/\text{\AA}^2$ (figure 6(c,d)). The dashed lines show the results obtained for unpolarized radiation.

In figures 6(a-d) the lines are concentrated in four groups: the main photoline A from the $4p$ -shell ionization of neutral Kr; lines from ionization of $\text{Kr}^+ 4s^2 4p^5$ mostly (B–D,F); from ionization of $\text{Kr}^{2+} 4s^2 4p^4$ mostly (G–L); ionization from $4s$ -shell of $\text{Kr}^{2+} 4s^2 4p^4$ and $\text{Kr}^{2+} 4s^1 4p^5$ (M–S).

For low-intensity regime (figure 6(a)) polarization suppresses line B and completely demolish it at $\omega = 80$ eV (figure 6(b)). That is because $\text{Kr}^+ 4s^2 4p^5 2P$ is completely polarized ($A_2(P) = -\sqrt{2}$) in the region of Cooper minimum and the polarization does not allow ionization to s -wave (rule 23). Lines G, H and M demonstrate similar behaviour, but at this intensity they are difficult to see.

The case of higher fluence (figure 6(c,d)) is more interesting. Besides overall increasing of the multiple ionization contributions which appears in enlarging peaks for binding energy above 30 eV and decreasing above discussed lines B, G, H and M, there are some lines which increase or even appear in comparison with unpolarized case. That are line F which can be distinguished only for polarized radiation, and lines J and N. The re-distribution is caused by enhanced contributions from ionization of S -terms, when ionization of P -terms suppressed by polarization.

Figure 7 shows the fluence dependence of the intensities of the spectral lines. The curves clearly indicate the

one-, two- and three-photon origin of the spectral features A and E; B–D, F, I, K; and G, H, J, L–S, respectively. The saturation appears at fluence above $100 \text{ ph}/\text{\AA}^2$, and the more pronounced the more number of photons involved. The figure shows that accounting of polarization does not change general multi-photon behaviour with intensity.

V. CONCLUSIONS

The role of the polarization both of the radiation and ionic states in sequential multiple ionization is studied theoretically. The system of equations similar to conventional rate equations for states population is formulated in terms of the statistical tensors. It is applicable to linearly and circularly polarized pulses for systems with well-separated (excited incoherently) levels within dipole approximation.

The method was applied to multiple ionization of Kr in the 65–80 eV region. Ionic states evolution, yields and photoelectron spectrum were calculated and compared for the linearly polarized and unpolarized radiation. Redistribution of ionic yields up to 10% of total amount and noticeable re-arrangement of photoelectron spectrum caused by polarization are predicted. In low-intensity regime polarization suppresses or even demolishes some photolines; in high-intensity regime polarization may emphasize structure of spectra and some lines become distinguishable only for polarized radiation.

It is shown that doubly hollow ionic states which can decay only via spontaneous emission are created more efficiently if a sample is irradiated by polarized radiation than by unpolarized. These hollow ion states are of particular interest because they can serve as a target to create autoionizing states of very exotic configuration.

The present study is a necessary point before accounting for the complex evolution of the system due to different opening Auger decay channels which become possible when $3d$ -shell ionization comes into play.

The research was funded by the Russian Foundation for Basic Research (RFBR) under project No. 20-52-12023 and Ministry of Science and Higher Education of the Russian Federation grant No. 075-15-2021-1353. The work of M.D.K. is supported by the Ministry of Science and Higher Education of the Russian Federation (project No. 0818-2020-0005) using resources of the Shared Services “Data Center of the Far-Eastern Branch of the Russian Academy of Sciences”.

-
- [1] K. Nass, L. Foucar, T. R. M. Barends, E. Hartmann, S. Botha, R. L. Shoeman, R. B. Doak, R. Alonso-Mori, A. Aquila, S. Bajt, A. Barty, R. Bean, K. R. Beyerlein, M. Bublitz, N. Drachmann, J. Gregersen, H. O. Jansson, W. Kabsch, S. Kassemeyer, J. E. Koglin, M. Krumrey, D. Mattle, M. Messerschmidt, P. Nissen, L. Reinhard, O. Sitsel, D. Sokaras, G. J. Williams, S. Hau-Riege, N. Timneanu, C. Caleman, H. N. Chapman, S. Boutet, and I. Schlichting, Indications of radiation damage in ferredoxin microcrystals using high-intensity X-FEL beams, *Journal of Synchrotron Radiation* **22**, 225 (2015).
- [2] L. Galli, S.-K. Son, M. Klinge, S. Bajt, A. Barty, R. Bean, C. Betzel, K. R. Beyerlein, C. Caleman,

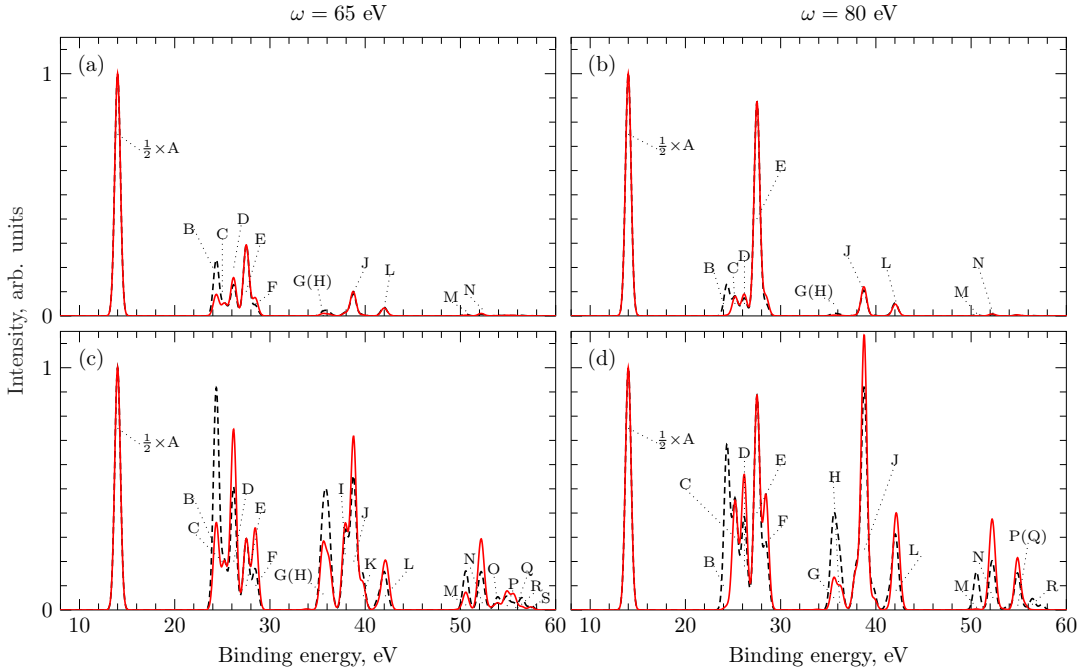


FIG. 6. Photoelectron spectrum for different photon energy: $\omega = 65$ eV ((a) for $F = 100$ ph/ \AA^2 , (c) for $F = 1000$ ph/ \AA^2), and $\omega = 80$ eV ((b) for $F = 100$ ph/ \AA^2 , (d) for $F = 1000$ ph/ \AA^2). The solid lines correspond to calculations for linearly polarized radiation, the dashed lines – to unpolarized radiation. The spectra are normalized in such a way that $1/2$ of the main line A equals unity. The spectral features are indicated by capital letters in accordance with Table I.

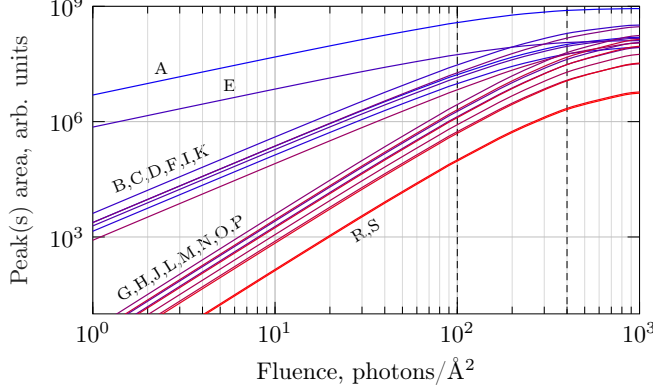


FIG. 7. Intensity dependence of different photoelectron lines on the fluence F at the photon energy $\omega = 65$ eV. The vertical dashed lines indicate fluences related to figures 3–6: 100 ph/ \AA^2 and 400 ph/ \AA^2 .

R. B. Doak, M. Duszenko, H. Fleckenstein, C. Gati, B. Hunt, R. A. Kirian, M. Liang, M. H. Nanao, K. Nass, D. Oberthur, L. Redecke, R. Shoeman, F. Stellato, C. H. Yoon, T. A. White, O. Yefanov, J. Spence, and H. N. Chapman, Electronic damage in s atoms in a native protein crystal induced by an intense x-ray free-electron laser pulse, *Structural Dynamics* **2**, 041703 (2015), <https://doi.org/10.1063/1.4919398>.

- [3] A. A. Sorokin, S. V. Bobashev, T. Feigl, K. Tiedtke, H. Wabnitz, and M. Richter, Photoelectric effect at ultrahigh intensities, *Phys. Rev. Lett.* **99**, 213002 (2007).
- [4] M. Kübel, C. Burger, N. G. Kling, T. Pischke, L. Beaufore, I. Ben-Itzhak, G. G. Paulus, J. Ullrich, T. Pfeifer, R. Moshammer, M. F. Kling, and B. Bergues, Complete characterization of single-cycle double ionization of argon from the nonsequential to the sequential ionization regime, *Phys. Rev. A* **93**, 053422 (2016).
- [5] R. Moshammer, Y. H. Jiang, L. Foucar, A. Rudenko, T. Ergler, C. D. Schröter, S. Lüdemann, K. Zrost, D. Fischer, J. Titze, T. Jahnke, M. Schöffler, T. Weber, R. Dörner, T. J. M. Zouros, A. Dorn, T. Ferger, K. U. Kühnel, S. Düsterer, R. Treusch, P. Radcliffe, E. Plönjes, and J. Ullrich, Few-photon multiple ionization of ne and ar by strong free-electron-laser pulses, *Phys. Rev. Lett.* **98**, 203001 (2007).
- [6] E. P. Kanter, B. Krässig, Y. Li, A. M. March, P. Ho, N. Rohringer, R. Santra, S. H. Southworth, L. F. Di-Mauro, G. Doumy, C. A. Roedig, N. Berrah, L. Fang, M. Hoener, P. H. Bucksbaum, S. Ghimire, D. A. Reis, J. D. Bozek, C. Bostedt, M. Messerschmidt, and L. Young, Unveiling and driving hidden resonances with high-fluence, high-intensity x-ray pulses, *Phys. Rev. Lett.* **107**, 233001 (2011).
- [7] M. Fushitani, Y. Sasaki, A. Matsuda, H. Fujise, Y. Kawabe, K. Hashigaya, S. Owada, T. Togashi, K. Nakajima, M. Yabashi, Y. Hikosaka, and A. Hishikawa, Multielectron-ion coincidence spectroscopy of xe in extreme ultraviolet laser fields: Nonlinear multiple ionization via double core-hole states, *Phys. Rev.*

- Lett. **124**, 193201 (2020).
- [8] L. Young, E. P. Kanter, B. Krässig, Y. Li, A. M. March, S. T. Pratt, R. Santra, S. H. Southworth, N. Rohringer, L. F. DiMauro, G. Doumy, C. A. Roedig, N. Berrah, L. Fang, M. Hoener, P. H. Bucksbaum, J. P. Cryan, S. Ghimire, J. M. Głownia, D. A. Reis, J. D. Bozek, C. Bostedt, and M. Messerschmidt, Femtosecond electronic response of atoms to ultra-intense X-rays, Nat. **466**, 56 (2010).
 - [9] N. Gerken, S. Klumpp, A. A. Sorokin, K. Tiedtke, M. Richter, V. Bürk, K. Mertens, P. Juranić, and M. Martins, Time-dependent multiphoton ionization of xenon in the soft-x-ray regime, Phys. Rev. Lett. **112**, 213002 (2014).
 - [10] M. Richter, S. V. Bobashev, A. A. Sorokin, and K. Tiedtke, Multiphoton ionization of atoms with soft x-ray pulses, Journal of Physics B: Atomic, Molecular and Optical Physics **43**, 194005 (2010).
 - [11] S. Klumpp, N. Gerken, K. Mertens, M. Richter, B. Sonntag, A. A. Sorokin, M. Braune, K. Tiedtke, P. Zimmermann, and M. Martins, Multiple auger cycle photoionisation of manganese atoms by short soft x-ray pulses, New Journal of Physics **19**, 043002 (2017).
 - [12] N. Berrah, L. Fang, T. Osipov, B. Murphy, C. Bostedt, and J. Bozek, Multiphoton ionization and fragmentation of molecules with the lclsx-ray fel, Journal of Electron Spectroscopy and Related Phenomena **196**, 34 (2014).
 - [13] H. Fukuzawa, S.-K. Son, K. Motomura, S. Mondal, K. Nagaya, S. Wada, X.-J. Liu, R. Feifel, T. Tachibana, Y. Ito, M. Kimura, T. Sakai, K. Matsunami, H. Hayashita, J. Kajikawa, P. Johnsson, M. Siano, E. Kukk, B. Rudek, B. Erk, L. Foucar, E. Robert, C. Miron, K. Tono, Y. Inubushi, T. Hattori, M. Yabashi, M. Yao, R. Santra, and K. Ueda, Deep inner-shell multiphoton ionization by intense x-ray free-electron laser pulses, Phys. Rev. Lett. **110**, 173005 (2013).
 - [14] S. H. Southworth, R. W. Dunford, D. Ray, E. P. Kanter, G. Doumy, A. M. March, P. J. Ho, B. Krässig, Y. Gao, C. S. Lehmann, A. Picón, L. Young, D. A. Walko, and L. Cheng, Observing pre-edge k-shell resonances in kr, xe, and xef₂, Phys. Rev. A **100**, 022507 (2019).
 - [15] M. Kurka, A. Rudenko, L. Foucar, K. U. Künnel, Y. H. Jiang, T. Ergler, T. Havermeier, M. Smolarski, S. Schössler, K. Cole, M. Schöffler, R. Dörner, M. Gensch, S. Düsterer, R. Treusch, S. Fritzsche, A. N. Grum-Grzhimailo, E. V. Gryzlova, N. M. Kabachnik, C. D. Schröter, R. Moshammer, and J. Ullrich, Two-photon double ionization of Ne by free-electron laser radiation: a kinematically complete experiment, J. Phys. B: At. Mol. Opt. Ph. **42**, 141002 (2009).
 - [16] M. Braune, G. Hartmann, M. Ilchen, A. Knie, T. Lischke, A. Reinköster, A. Meissner, S. Deinert, L. Glaser, O. Al-Dossary, A. Ehresmann, A. S. Kheifets, and J. Viefhaus, Electron angular distributions of noble gases in sequential two-photon double ionization, J. Mod. Opt. **63**, 324 (2016).
 - [17] P. A. Carpeggiani, E. V. Gryzlova, M. Reduzzi, A. Dubrouil, D. Faccialá, M. Negro, K. Ueda, S. M. Burkov, F. Frassetto, F. Stienkemeier, Y. Ovcharenko, M. Meyer, O. Plekan, P. Finetti, K. C. Prince, C. Callegari, A. N. Grum-Grzhimailo, and G. Sansone, Complete reconstruction of bound and unbound electronic wavefunctions in two-photon double ionization, Nat. Phys. **15**, 170 (2019).
 - [18] T. Mazza, M. Ilchen, M. D. Kiselev, E. V. Gryzlova, T. M. Baumann, R. Boll, A. De Fanis, P. Grychtol, J. Montaño, V. Music, Y. Ovcharenko, N. Rennhack, D. E. Rivas, P. Schmidt, R. Wagner, P. Ziolkowski, N. Berrah, B. Erk, P. Johnsson, C. Küstner-Wetekam, L. Marder, M. Martins, C. Ott, S. Pathak, T. Pfeifer, D. Rolles, O. Zatsarinny, A. N. Grum-Grzhimailo, and M. Meyer, Mapping resonance structures in transient core-ionized atoms, Phys. Rev. X **10**, 041056 (2020).
 - [19] A. S. Kheifets, Sequential two-photon double ionization of noble gas atoms, Journal of Physics B: Atomic, Molecular and Optical Physics **40**, F313 (2007).
 - [20] A. N. Grum-Grzhimailo, E. V. Gryzlova, S. Fritzsche, and N. M. Kabachnik, Photoelectron angular distributions and correlations in sequential double and triple atomic ionization by free electron lasers, Journal of Modern Optics **63**, 334 (2016), <https://doi.org/10.1080/09500340.2015.1047805>.
 - [21] S. Mondal, R. Ma, K. Motomura, H. Fukuzawa, A. Yamada, K. Nagaya, S. Yase, Y. Mizoguchi, M. Yao, A. Rouzee, A. Hundertmark, M. J. J. Vrakking, P. Johnsson, M. Nagasono, K. Tono, T. Togashi, Y. Senba, H. Ohashi, M. Yabashi, T. Ishikawa, I. P. Sazhina, S. Fritzsche, N. M. Kabachnik, and K. Ueda, Photoelectron angular distributions for the two-photon sequential double ionization of xenon by ultrashort extreme ultraviolet free electron laser pulses, Journal of Physics B: Atomic, Molecular and Optical Physics **46**, 164022 (2013).
 - [22] M. Ilchen, G. Hartmann, E. V. Gryzlova, A. Achner, E. Allaria, A. Beckmann, M. Braune, J. Buck, C. Callegari, R. N. Coffee, R. Cucini, M. Danailov, A. De Fanis, A. Demidovich, E. Ferrari, P. Finetti, L. Glaser, A. Knie, A. O. Lindahl, O. Plekan, N. Mahne, T. Mazza, L. Raimondi, E. Roussel, F. S. J. Seltmann, I. Shevchuk, C. Svetina, P. Walter, M. Zangrandi, J. Viefhaus, A. N. Grum-Grzhimailo, and M. Meyer, Symmetry breakdown of electron emission in extreme ultraviolet photoionization of argon, Nat. Commun. **8**, 4659 (2018).
 - [23] S. Augustin, M. Schulz, G. Schmid, K. Schnorr, E. V. Gryzlova, H. Lindenblatt, S. Meister, Y. F. Liu, F. Trost, L. Fechner, A. N. Grum-Grzhimailo, S. M. Burkov, M. Braune, R. Treusch, M. Gisselbrecht, C. D. Schröter, T. Pfeifer, and R. Moshammer, Signatures of autoionization in the angular electron distribution in two-photon double ionization of ar, Phys. Rev. A **98**, 033408 (2018).
 - [24] A. Rouzee, P. Johnsson, E. Gryzlova, H. Fukuzawa, A. Yamada, W. Siu, Y. Huismans, E. Louis, F. Bijkerk, D. Holland, A. Grum-Grzhimailo, N. Kabachnik, M. Vrakking, and K. Ueda, Angle-resolved photoelectron spectroscopy of sequential three-photon triple ionization of neon at 90.5 ev photon energy, Phys. Rev. A **83**, 031401(R) (2011).
 - [25] N. M. Kabachnik, S. Fritzsche, A. N. Grum-Grzhimailo, M. Meyer, and K. Ueda, Coherence and correlations in photoinduced auger and fluorescence cascades in atoms, Phys. Rep. **451**, 155 (2007).
 - [26] P. O'Keeffe, E. V. Gryzlova, D. Cubaynes, G. A. Garcia, L. Nahon, A. N. Grum-Grzhimailo, and M. Meyer, Isotopically resolved photoelectron imaging unravels complex atomic autoionization dynamics by two-color resonant ionization, Phys. Rev. Lett. **111**, 243002 (2013).
 - [27] P. Wernet, J. Schulz, B. Sonntag, K. Godehusen, P. Zim-

- ermann, A. N. Grum-Grzhimailo, N. M. Kabachnik, and M. Martins, *2p* photoelectron spectra and linear alignment dichroism of atomic cr, *Phys. Rev. A* **64**, 042707 (2001).
- [28] M. Meyer, A. N. Grum-Grzhimailo, D. Cubaynes, Z. Felffi, E. Heinecke, S. T. Manson, and P. Zimmermann, Magnetic dichroism in *k*-shell photoemission from laser excited li atoms, *Phys. Rev. Lett.* **107**, 213001 (2011).
- [29] M. Wedowski, K. Godehusen, F. Weisbarth, P. Zimmermann, M. Martins, T. Dohrmann, A. von dem Borne, B. Sonntag, and A. N. Grum-Grzhimailo, Vacuum-ultraviolet photoelectron spectroscopy of laser-excited aligned ca atomsin the 3p-3d resonance region, *Phys. Rev. A* **55**, 1922 (1997).
- [30] M. Ilchen, N. Douguet, T. Mazza, A. J. Rafipoor, C. Callegari, P. Finetti, O. Plekan, K. C. Prince, A. Demidovich, C. Grazioli, L. Avaldi, P. Bolognesi, M. Coreno, M. Di Fraia, M. Devetta, Y. Ovcharenko, S. Düsterer, K. Ueda, K. Bartschat, A. N. Grum-Grzhimailo, A. V. Bozhevolnov, A. K. Kazansky, N. M. Kabachnik, and M. Meyer, Circular dichroism in multiphoton ionization of resonantly excited He^+ ions, *Phys. Rev. Lett.* **118**, 013002 (2017).
- [31] D. Cubaynes, M. Meyer, A. N. Grum-Grzhimailo, J.-M. Bizau, E. T. Kennedy, J. Bozek, M. Martins, S. Cantton, B. Rude, N. Berrah, and F. J. Wuilleumier, Dynamically and quasiforbidden transitions in photoionization of open-shell atoms: A combined experimental and theoretical study, *Phys. Rev. Lett.* **92**, 233002 (2004).
- [32] W. Nörtershäuser, A. Surzhykov, R. Sánchez, B. Botermann, G. Gwinner, G. Huber, S. Karpuk, T. Kühl, C. Novotny, S. Reinhardt, G. Saathoff, T. Stöhlker, and A. Wolf, Polarization-dependent disappearance of a resonance signal: Indication for optical pumping in a storage ring?, *Phys. Rev. Accel. Beams* **24**, 024701 (2021).
- [33] E. T. Karamatskos, D. Markellos, and P. Lambropoulos, Multiple ionization of argon under 123 eV FEL radiation and the creation of 3s-hollow ions, *Journal of Physics B: Atomic, Molecular and Optical Physics* **46**, 164011 (2013).
- [34] T. Nakajima and L. A. A. Nikolopoulos, Use of helium double ionization for autocorrelation of an xuv pulse, *Phys. Rev. A* **66**, 041402R (2002).
- [35] M. G. Makris, P. Lambropoulos, and A. Mihelič, Theory of multiphoton multielectron ionization of xenon under strong 93-eV radiation, *Phys. Rev. Lett.* **102**, 033002 (2009).
- [36] S.-K. Son and R. Santra, Impact of hollow-atom formation on coherent x-ray scattering at high intensity, *Phys. Rev. A* **83**, 033402 (2011).
- [37] S.-K. Son and R. Santra, Monte Carlo calculation of ion, electron, and photon spectra of xenon atoms in x-ray free-electron laser pulses, *Phys. Rev. A* **85**, 063415 (2012).
- [38] U. Lorenz, N. M. Kabachnik, E. Weckert, and I. A. Vartanyants, Impact of ultrafast electronic damage in single-particle x-ray imaging experiments, *Phys. Rev. E* **86**, 051911 (2012).
- [39] V. Y. Lunin, A. N. Grum-Grzhimailo, E. V. Gryzlova, D. O. Sinitsyn, T. E. Petrova, N. L. Lunina, N. K. Balabaev, K. B. Tereshkina, A. S. Stepanov, and Y. F. Krupyanskii, Efficient calculation of diffracted intensities in the case of nonstationary scattering by biological macromolecules under XFEL pulses, *Acta Cryst. D* **71**, 293 (2015).
- [40] S. Serkez, G. Geloni, S. Tomin, G. Feng, E. V. Gryzlova, A. N. Grum-Grzhimailo, and M. Meyer, Overview of options for generating high-brightness attosecond x-ray pulses at free-electron lasers and applications at the European XFEL, *J. Opt.* **20**, 024005 (2018).
- [41] C. Butth, R. Beerwerth, R. Obaid, N. Berrah, L. S. Cederbaum, and S. Fritzsche, Neon in ultrashort and intense x-rays from free electron lasers, *J. Phys. B: At. Mol. Opt. Ph.* **51**, 055602 (2018).
- [42] G. C. King, M. Tronc, F. H. Read, and R. C. Bradford, An investigation of the structure near the $l_{2,3}$ edges of argon, the $m_{4,5}$ edges of krypton and the $n_{4,5}$ edges of xenon, using electron impact with high resolution, *J. Phys. B: At. Mol. Ph.* **10**, 2479 (1977).
- [43] M. Ilchen, T. Mazza, E. T. Karamatskos, D. Markellos, S. Bakhtiarzadeh, A. J. Rafipoor, T. J. Kelly, N. Walsh, J. T. Costello, P. O'Keeffe, N. Gerken, M. Martins, P. Lambropoulos, and M. Meyer, Two-electron processes in multiple ionization under strong soft-x-ray radiation, *Phys. Rev. A* **94**, 013413 (2016).
- [44] E. V. Gryzlova, M. D. Kiselev, M. M. Popova, A. A. Zubekhin, G. Sansone, and A. N. Grum-Grzhimailo, Multiple sequential ionization of valence $n = 4$ shell of krypton by intense femtosecond xuv pulses, *Atoms* **8**, 10.3390/atoms8040080 (2020).
- [45] NIST Atomic Spectra Database (version 5.8). Available: <https://physics.nist.gov/asd> [May 18 2020]. National Institute of Standards and Technology, Gaithersburg, MD (2020).
- [46] V. V. Balashov, A. N. Grum-Grzhimailo, and . M. Kabachnik, *Polarization and Correlation Phenomena in Atomic Collisions. A Practical Theory Course* (Kluwer Plenum, New York, 2000).
- [47] K. Blum, *Density Matrix Theory and Applications* (Plenum, New York, 1996).
- [48] E. Allaria, R. Appio, L. Badano, W. A. Barletta, S. Basanese, S. G. Biedron, A. Borga, E. Busetto, D. Castronovo, P. Cinquegrana, S. Cleva, D. Cocco, M. Cornacchia, P. Craievich, I. Cudin, G. D'Auria, M. Dal Forno, M. B. Danailov, R. De Monte, G. De Ninno, P. Delgiusto, A. Demidovich, S. Di Mitri, B. Diviacco, A. Fabris, R. Fabris, W. Fawley, M. Ferianis, E. Ferrari, S. Ferry, L. Froehlich, P. Furlan, G. Gaio, F. Gelmetti, L. Giannessi, M. Giannini, R. Gobessi, R. Ivanov, E. Karantzoulis, M. Lonza, A. Lutman, B. Mahieu, M. Milloch, S. V. Milton, M. Musardo, I. Nikolov, S. Noe, F. Parmigiani, G. Penco, M. Petronio, L. Pivetta, M. Predonzani, F. Rossi, L. Rumiz, A. Salom, C. Scafuri, C. Serpico, P. Sigalotti, S. Spampinati, C. Spezzani, M. Svandrlík, C. Svetina, S. Tazzari, M. Trovo, R. Umer, A. Vascotto, M. Veronese, R. Visintini, M. Zaccaria, D. Zangrandi, and M. Zangrandi, Highly coherent and stable pulses from the FERMI seeded free-electron laser in the extreme ultraviolet, *Nat. Photonics* **6**, 699 (2012).
- [49] P. Finetti, H. Höppner, E. Allaria, C. Callegari, F. Capotondi, P. Cinquegrana, M. Coreno, R. Cucini, M. B. Danailov, A. Demidovich, G. De Ninno, M. Di Fraia, R. Feifel, E. Ferrari, L. Fröhlich, D. Gauthier, T. Golz, C. Grazioli, Y. Kai, G. Kurdi, N. Mahne, M. Manfredda, N. Medvedev, I. P. Nikolov, E. Pedersoli, G. Penco, O. Plekan, M. J. Prandolini, K. C. Prince, L. Raimondi, P. Rebernik, R. Riedel, E. Roussel, P. Sigalotti, R. Squibb, N. Stojanovic, S. Stranges, C. Svetina, T. Tanikawa, U. Teubner, V. Tkachenko, S. Toleikis,

- M. Zangrande, B. Ziaja, F. Tavella, and L. Giannessi, Pulse duration of seeded free-electron lasers, Phys. Rev. X **7**, 021043 (2017).
- [50] O. Zatsarinny, BSR: B-spline atomic R-matrix codes, Comput. Phys. Commun. **174**, 273 (2006).
- [51] U. Kleiman and B. Lohmann, Photoionization of closed-shell atoms: Hartree-fock calculations of orientation and alignment, Journal of Electron Spectroscopy and Related Phenomena **131-132**, 29 (2003).
- [52] M. Amusia, L. Chernysheva, and V. Yarzhemsky, *Handbook of theoretical atomic physics: data for photon absorption, electron scattering, and vacancies decay* (Springer Science & Business Media, 2012).
- [53] W. R. Johnson and K. T. Cheng, Photoionization of the outer shells of neon, argon, krypton, and xenon using the relativistic random-phase approximation, Phys. Rev. A **20**, 978 (1979).
- [54] K.-N. Huang, W. Johnson, and K. Cheng, Theoretical photoionization parameters for the noble gases argon, krypton, and xenon, Atomic Data and Nuclear Data Tables **26**, 33 (1981).
- [55] S. Aksela, H. Aksela, M. Levasalmi, K. H. Tan, and G. M. Bancroft, Partial photoionization cross sections of kr 3d, 4s, and 4p levels in the photon energy range 37–160 ev, Phys. Rev. A **36**, 3449 (1987).
- [56] M. Y. Amusia, V. K. Ivanov, N. A. Cherepkov, and L. V. Chernysheva, Interference effects in photoionization of noble gas atoms outer s-shells, Physics Letters **40A**, 361 (1972).
- [57] N. Berrah, A. Farhat, B. Langer, B. M. Lagutin, P. V. Demekhin, I. D. Petrov, V. L. Sukhorukov, R. Wehlitz, S. B. Whitfield, J. Viehaus, and U. Becker, Angle-resolved energy dependence of the $4p^4nd(^2S_{1/2})$ ($n = 4 - 7$) correlation satellites in kr from 38.5 to 250 ev: Experiment and theory, Phys. Rev. A **56**, 4545 (1997).
- [58] A. Ehresmann, F. Vollweiler, H. Schmoranzer, V. L. Sukhorukov, B. M. Lagutin, I. D. Petrov, G. Mentzel, and K.-H. Schartner, Photoionization of kr 4s: III. detailed and extended measurements of the kr 4s-electron ionization cross section, J. Phys. B: At. Mol. Opt. Ph. **27**, 1489 (1994).
- [59] S. Fritzsche, A. N. Grum-Grzhimailo, E. V. Gryzlova, and N. M. Kabachnik, Angular distributions and angular correlations in sequential two-photon double ionization of atoms, J. Phys. B: At. Mol. Opt. Ph. **41**, 165601 (2008).
- [60] S. Fritzsche, A. N. Grum-Grzhimailo, E. V. Gryzlova, and N. M. Kabachnik, Sequential two-photon double ionization of Kr atoms, J. Phys. B: At. Mol. Opt. Ph. **42**, 145602 (2009).
- [61] A. N. Grum-Grzhimailo, E. V. Gryzlova, and M. Meyer, Non-dipole effects in the angular distribution of photoelectrons in sequential two-photon atomic double ionization, J. Phys. B: At. Mol. Opt. Ph. **45**, 215602 (2012).
- [62] E. V. Gryzlova, A. N. Grum-Grzhimailo, S. Fritzsche, and N. M. Kabachnik, Angular correlations between two electrons emitted in the sequential two-photon double ionization of atoms, J. Phys. B: At. Mol. Opt. Ph. **43**, 225602 (2010).
- [63] M. D. Kiselev, P. A. Carpeggiani, E. V. Gryzlova, S. M. Burkov, M. Reduzzi, A. Dubrouil, D. Facciala, M. Negro, K. Ueda, F. Frassetto, F. Stienkemeier, Y. Ovcharenko, M. Meyer, M. D. Fraia, O. Plekan, K. C. Prince, and C. Callegari, Photoelectron spectra and angular distribution in sequential two-photon double ionization in the region of autoionizing resonances of arii and krii, J. Phys. B: At. Mol. Ph. **accepted** (2020).
- [64] M. J. Lynch, A. B. Gardner, K. Codling, and G. V. Marr, The photoionization of the 3s subshell of argon in the threshold region by photoelectron spectroscopy, Physics Letters **43A**, 237 (1973).
- [65] S. Mondal, R. Ma, K. Motomura, H. Fukuzawa, A. Yamada, K. Nagaya, S. Yase, Y. Mizoguchi, M. Yao, A. Rouzée, A. Hundertmark, M. J. J. Vrakking, P. Johnsson, M. Nagasano, K. Tono, T. Togashi, Y. Senba, H. Ohashi, M. Yabashi, T. Ishikawa, I. P. Sazhina, S. Fritzsche, N. M. Kabachnik, and K. Ueda, Photoelectron angular distributions for the two-photon sequential double ionization of xenon by ultrashort extreme ultraviolet free electron laser pulses, J. Phys. B: At. Mol. Opt. Phys **46**, 164022 (2013).
- [66] B. Rudek, S.-K. Son, L. Foucar, S. W. Epp, B. Erk, R. Hartmann, M. Adolph, R. Andritschke, A. Aquila, N. Berrah, C. Bostedt, J. Bozek, N. Coppola, F. Filsinger, H. Gorke, T. Gorkhover, H. Graafsma, L. Gumprecht, A. Hartmann, G. Hauser, S. Herrmann, H. Hirsemann, P. Holl, A. Hömke, L. Journel, C. Kaiser, N. Kimmel, F. Krasniqi, K.-U. Kühnle, M. Matysek, M. Messerschmidt, D. Miesner, T. Möller, R. Moshammer, K. Nagaya, B. Nilsson, G. Potdevin, D. Pietschner, C. Reich, D. Rupp, G. Schaller, I. Schlüting, C. Schmidt, F. Schopper, S. Schorb, C.-D. Schröter, J. Schulz, M. Simon, H. Soltau, L. Strüder, K. Ueda, G. Weidenspointner, R. Santra, J. Ullrich, A. Rudenko, and D. Rolles, Ultra-efficient ionization of heavy atoms by intense x-ray free-electron laser pulses, Nature Photonics **6**, 858 (2012).
- [67] B. Rudek, D. Rolles, S.-K. Son, L. Foucar, B. Erk, S. Epp, R. Boll, D. Anielski, C. Bostedt, S. Schorb, R. Coffee, J. Bozek, S. Trippel, T. Marchenko, M. Simon, L. Christensen, S. De, S.-i. Wada, K. Ueda, I. Schlüting, R. Santra, J. Ullrich, and A. Rudenko, Resonance-enhanced multiple ionization of krypton at an x-ray free-electron laser, Phys. Rev. A **87**, 023413 (2013).
- [68] J. A. R. Samson and J. L. Gardner, Photoionization cross sections of the outer s-subshell electrons in the rare gases, Phys. Rev. Lett. **33**, 671 (1974).
- [69] V. L. Sukhorukov, B. M. Lagutin, I. D. Petrov, H. Schmoranzer, A. Ehresmann, and K. H. Schartner, Photoionization of kr near 4s threshold. II. intermediate-coupling theory, J. Phys. B: At. Mol. Opt. Ph. **27**, 241 (1994).
- [70] J. Tulkki, S. Aksela, H. Aksela, E. Shigemasa, A. Yagishita, and Y. Furusawa, Krypton 4p, 4s, and 3d partial photoionization cross sections below a photon energy of 260 ev, Phys. Rev. A **45**, 4640 (1992).
- [71] L. A. A. Nikolopoulos, Time-dependent theory of angular correlations in sequential double ionization, Phys. Rev. Lett. **111**, 093001 (2013).
- [72] E. V. Gryzlova, R. Ma, H. Fukuzawa, K. Motomura, A. Yamada, K. Ueda, A. N. Grum-Grzhimailo, N. M. Kabachnik, S. I. Strakhova, A. Rouzée, A. Hundertmark, M. J. J. Vrakking, P. Johnsson, K. Nagaya, S. Yase, Y. Mizoguchi, M. Yao, M. Nagasano, K. Tono, T. Togashi, Y. Senba, H. Ohashi, M. Yabashi, and T. Ishikawa, Doubly resonant three-photon double ionization of ar atoms induced by an euv free-electron laser, Phys. Rev. A **84**, 063405 (2011).
- [73] S. Shwartz, M. Fuchs, J. B. Hastings, Y. Inubushi,

- T. Ishikawa, T. Katayama, D. A. Reis, T. Sato, K. Tono, M. Yabashi, S. Yudovich, and S. E. Harris, X-ray second harmonic generation, Phys. Rev. Lett. **112**, 163901 (2014).
- [74] B. Kettle, A. Aquila, S. Boutet, P. H. Bucksbaum, G. Carini, Y. Feng, E. Gamboa, S. Ghimire, S. Glenzer, P. Hart, J. B. Hastings, T. Henighan, M. Hunter, J. Koglin, M. Kozina, H. Liu, M. J. MacDonald, M. Trigo, D. A. Reis, and M. Fuchs, Anomalous two-photon compton scattering, New Journal of Physics **23**, 115008 (2021).